

Globulin-p and 11S-Globulin from *Amaranthus Hypochondriacus*: are Two Isoforms of the 11S-Globulin

Alejandra Quiroga · E. Nora Martínez ·
Hélène Rogniaux · Audrey Geairon ·
M. Cristina Añón

Published online: 17 November 2009
© Springer Science+Business Media, LLC 2009

Abstract Amaranth is an ancient crop with a high content of good quality proteins. Globulins are some of the most abundant storage proteins of amaranth grain. They contain two fractions distinguishable according to their different solubility: the salt-soluble 7S and 11S-globulins and the globulin-p soluble in mild-alkaline, low-ionic-strength solutions. As part of the amaranth proteins characterization, in this work we investigated the structural characteristics responsible for the different physicochemical properties of these globulins. We studied certain conformational parameters of the purified aggregates (AMGp) and individual molecules (IMGp) of globulin-p and of the partially purified globulin (ppGb) and compared the AMGp polypeptide sequences with the sequence of the 11S-globulin propolypeptide from *Amaranthus* (gil122726601). The results indicated that the AMGp aggregates are responsible for the different solubility of globulin-p. Subtle conformational differences as determined by fluorescence

spectroscopy and urea sensitivity were found between the molecules studied: The AMGp showed some surface differences from the IMGp and the ppGb; the AMGp also had a lower affinity for the hydrophobic fluorescent probe 1,8-aniline-naphthalene-sulfonate and a higher ionic charge than the ppGb and the IMGp, characteristics that might cause their lower solubility. In addition, we have demonstrated differences between the AMGp polypeptide sequences and that reported for amaranth 11S-globulin. These differences suggest that the globulin-p and 11S-globulin are two 11S-globulin isoforms comprised of polypeptides coming from different legumin-gene subfamilies.

Keywords Amaranth proteins · Protein structure · Storage proteins · Globulin

Abbreviations

Gp	Crude globulin-p fraction
AMGp	Purified globulin-p aggregated molecules
IMGp	Purified globulin-p individual molecules (280 kDa)
Gb	Crude salt soluble globulin fraction
ppGb	Partially purified salt soluble-globulins
CHAPS	3-[(3-cholamidopropyl)-dimethyl-ammonio]-1-propane sulfonate
DTT	Dithiothreitol
IEF	Isoelectric focusing
IPG	Immobilized pH gradient
ANS	1,8-Aniline-naphthalene-sulfonate
A and (B, B')	Globulin-p, acid and basic polypeptides, respectively

A. Quiroga · E. N. Martínez (✉) · M. C. Añón
Facultad de Ciencias Exactas, Centro de Investigación y
Desarrollo en Criotecnología de Alimentos (CIDCA),
Universidad Nacional de La Plata y Consejo Nacional de
Investigaciones Científicas y Técnicas, calle 47 y 116,
1900 La Plata, Argentina
e-mail: noramar@quimica.unlp.edu.ar

A. Quiroga
e-mail: aquiroga@quimica.unlp.edu.ar

H. Rogniaux · A. Geairon
UR1268 Biopolymères Interactions Assemblages, Plate-Forme
BIBS, INRA, 44300 Nantes, France

M	Globulin-p propolypeptide
MALDI-MS	Matrix-assisted laser desorption ionization mass spectrometry
TOF	Time of flying
IEF → SDS-PAGE	Two-dimensional isoelectric focussing polyacrylamide-gel electrophoresis
LC-MS/MS	Nanoscale capillary-liquid chromatography–tandem mass spectrometry
ND-PAGE	Non-denaturing polyacrylamide-gel electrophoresis

1 Introduction

The globulins as a class represent the main storage proteins in dicotyledonous plants. As with all storage proteins, the globulin structure must fulfil two conditions necessary for its function: the molecules must have an appropriate structural conformation for efficient and maximal packing within protein vacuoles and be a good substrate for the particular endoproteases that will hydrolyze it during the course of germination. Amaranth is a pseudocereal with a high content of good quality proteins. The amaranth globulins comprise the salt-soluble species—the 11S-globulin and the 7S-globulin-like protein—along with the globulin-p (Gp), soluble in mild-alkaline, low-ionic-strength solutions. According to the classification based on gene structure, the amaranth glutelins must also be considered globulins [12].

The secondary and tertiary structures of the purified 7S and 11S-globulins were studied by [19, 22]. Using far-ultraviolet circular dichroism they found that both globulins contained a larger fraction of beta sheets (35–71%) than alpha-helices (around 7%) and by means of near-ultraviolet-circular-dichroism analysis they concluded that within the structure of the 7S-globulin-like protein the aromatic groups are either distant from one another or else highly motile compared to those of the 11S-globulin. Studies by means of electron microscopy and computer-image analysis [20] supported a model for the 11S-globulin consisting in a dodecameric structure with its constituent subunits arranged in two annular hexagonal rings, just as had been described for other legumins [2, 31]. Studies on the sequence of the amaranth 11S proglobulin confirmed that this globulin is synthesized, as with other legumins, from a precursor that is processed and sorted into vacuoles [6, 25, 30].

The conformation of non-purified globulins and the influence of pH, ionic strength, and denaturants on their

stability were studied by means of differential scanning calorimetry, circular dichroism, intrinsic fluorescence, surface-hydrophobicity determination, and immunochemical techniques [3, 8–10, 13, 14, 16, 21, 24, 34]. Both the 11S-globulin and the Gp are legumin-like proteins with similar polypeptide compositions [5, 11, 24, 32, 33, 35, 37] and a high thermostability (denaturation temperature at around 90 °C), but subtle differences were found between these two globulins [16, 24, 32]. The Gp was found to stay in a mostly polymerized form, but its individual molecules (IMGp) are of the same molecular weight as the 11S-globulin, though the cause of this difference is still unknown. Gp molecules contain a greater amount of the non-processed propolypeptide [1, 6, 10, 24, 33] partially exposed on the molecular surface [3], a finding that led to the proposal that this feature might be one of the structural characteristics responsible for the globulin's tendency to polymerize.

The compactness of Gp in its aggregated state fulfils the condition of maximal packing capability, while the presence of large amounts of the non-processed polypeptide gives the globulin a high susceptibility to protease action that enables a facile degradation during germination [4]. By contrast, the nonaggregated 11S-globulin with fewer propolypeptides was found to be hydrolyzed at the same time as the Gp during germination [4]. This result would indicate that the conformation of these two globulin isoforms fits in well with their biological function. Nevertheless, some conformational difference may exist between the Gp and the Gb that accounts for their quite different physicochemical properties [8, 24]. Although amaranth subunits from different subfamilies may be interchangeable among different oligomers, structural differences between the subunits (i.e., the nature of their polypeptides) might affect their assembly in such a way as to make them separate into molecules with different conformations. This hypothesis is supported by findings that indicate a different susceptibility of the propolypeptides of Gp and the 11S-globulin to the sunflower vacuolar-processing enzyme [26]. A comparison between the Gp polypeptide sequences and those of the reported 11S-globulin may also help to test that hypothesis.

To date there is no information about the conformational differences between the purified polymerized and individual molecules of the Gp and the partially purified Gb. With an aim at investigating the causes of the different physicochemical properties of those classes of amaranth globulin, we compared some of their surface and conformational parameters as well as the polypeptide sequences of the Gp protein and of the reported 11S-globulin [6]. These findings should shed further light on the structure-function relationship of plant storage proteins.

2 Materials and Methods

2.1 Plant Material

Seeds from *Amaranthus hypochondriacus* (commercial cultivar) were harvested at the Estación Experimental del Instituto Nacional de Investigaciones Forestales y Agropecuarias (INIFAP), Chapingo, México, and kindly provided to our laboratory in Argentina.

Flour was obtained by grinding whole seeds in a Udy™ mill (Facultad de Ciencias Agrarias y Forestales, Universidad Nacional de La Plata, Argentina) with a 1-mm mesh and then sieved through a 0.092-mm mesh. The flour was suspended in hexane at a concentration of 10% (w/v), defatted for 24 h with continuous stirring, air-dried at room temperature, and stored at 4 °C until use.

2.2 Protein Extraction

The salt-soluble globulins (Gb) and the Gp were extracted by a modification of the Osborne method [3]. The extraction was conducted at room temperature with a meal/solution ratio (w/v) of 1:10. The flour was treated twice with water to extract albumin and then twice with 32.5 mM K₂HPO₄, 2.6 mM KH₂PO₄, 0.4 M NaCl, pH 7.5 (buffer A) to extract the salt-soluble globulins. The Gp was extracted by treating the residue twice with water. After each treatment, the extracted residue was separated by centrifugation at 9,000g for 20 min at room temperature. The supernatants containing salt-soluble globulin and the Gp (either as a soluble or a dispersed protein) were each adjusted to pH 6 with 2 N HCl. The resulting precipitates were suspended in water, neutralized with 0.1 N NaOH, and freeze-dried.

2.3 Preparation of Partially Purified ppGb, AMGp, and IMGp

The ppGb and the components of the Gp—molecules of 280 kDa (individual molecules [IMGp]) and their aggregates of molecular mass >500 kDa (aggregated molecules [AMGp])—were prepared by gel filtration on a Sephacryl S-300 HR column (2.5 × 90 cm) with a fractionation range of 10–1,500 kDa as previously described by [18] with slight modifications. The column was packed and equilibrated with three bed volumes of 33.3 mM K₂HPO₄, 1.7 mM KH₂PO₄, pH 8.5 (buffer B) containing 0.02% (w/v) NaN₃.

A 4-mL sample containing 50 mg of protein was layered onto the gel-filtration column. Protein fractions were eluted from the column at room temperature (25 °C) at a flow rate of 0.58 mL/min obtained with a Gilson Minipuls 2 peristaltic pump. Profiles are shown in Fig. 1. Fractions (3 mL) were collected with a Buchler (Fractomete Alpha 400)

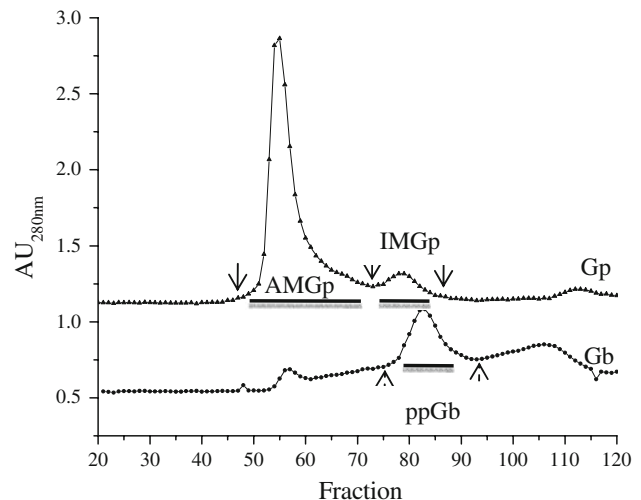


Fig. 1 Sephacryl S-300 gel filtration chromatography of crude globulin-p (*Gp*) and crude salt soluble globulins (*Gb*). Pooled fractions corresponding to *Gp* aggregates (*AMGp*), *Gp* individual molecules (*IMGp*) and partially purified salt soluble globulins (*ppGb*) are indicated in the figure

fraction collector and the absorbance of the fractions was measured at 280 nm. Fractions corresponding to the ppGb molecules and to IMGp and AMGp species were each pooled (Fig. 1) and, at a dilution of 1:100 in buffer, concentrated by means of an Amicon 8020 (Amicon Inc.) ultrafiltration cell, containing a 10-kDa pore membrane (Amicon, YM10). The resulting fractions were stored at –80 °C and freeze dried.

2.4 Solubility

The solubility of the globulin species the AMGp, IMGp, and ppGb was analyzed by preparing 0.1% (w/v) suspensions in buffer A or buffer B. Samples were incubated for 1 h at room temperature with vortexing every 15 min in a Termolyne Maxi Max. (Iowa, USA). Samples were then centrifuged at 10,000g for 30 min at 15 °C. The protein content in the supernatant was determined by the Lowry method and the protein solubility considered to be the amount of protein assayed in the supernatants as a percent of the total protein content of the sample.

2.5 Gel-Filtration Chromatography

The ppGb, the AMGp, and the IMGp in buffer B were analyzed by gel-filtration chromatography at room temperature. A Superose 6B HR 10/30 column was employed linked to a Pharmacia LKB, FPLC System (Uppsala, Sweden). Samples (4 mg of protein in 0.2 mL) were eluted with the same buffer in which they were prepared and the optical density at 280 nm was recorded. The column was

calibrated with gel filtration calibration kits HMW and LMW (GE-Healthcare, Buckinghamshire, UK).

Curves were processed and data evaluated through the use of the Pharmacia AB, FPLC director and FPLC assistant software.

2.6 ND-PAGE

Runs were carried out on 7% (w/v) acrylamide gels prepared in minislabs (Bio Rad Protean II Model). These tests were performed in the buffer system described by Martínez et al. [24]. Protein samples (20 mg/mL) were dissolved in 0.125 M Tris-HCl, (pH 8.8), 20% (v/v) glycerol, 0.05% (w/v) bromophenol blue and centrifuged at 15,800g for 5 min, at room temperature. The supernatants were separated and loaded on the gel (4–6 μ L/lane). Gels were fixed and stained with Coomassie Brilliant Blue.

2.7 Surface Hydrophobicity

The AMGp, IMGp, and ppGb parameters—surface hydrophobicity (Ho), the equilibrium-binding or affinity constant (K_a), and the number of exposed 1,8-aniline-naphthalene-sulfonate—(ANS) attachment sites per mg of protein (n)—were determined as described by [7] for the use of the ANS fluorescent probe (Aldrich Chemical Co.). The emission spectra (370–600 nm) of the samples in buffer B (0.05–0.15 mg/mL) equilibrated with different concentrations of ANS (from 0.0 to 83.5 μ M) were first generated and the fluorescence measurements then corrected by subtracting the corresponding blanks (ANS solutions alone at the same concentration as the sample) to obtain ΔFI , the increase in fluorescence as a result of ANS binding. The ΔFI at 470 nm (the maximum emission of an ANS-protein complex) was finally plotted against the ANS concentration (μ M) and the data adjusted to the following equation:

$$\Delta FI = \frac{A \times \text{ANS}}{B + \text{ANS}} \quad (1)$$

where the coefficients are $B = \frac{1}{K_a}$ and $A = \Delta FI_{\max}$ ($A = \Delta FI_{\max}$ is the fluorescence intensity at saturation).

Upon considering that ΔFI is proportional to the amount of ANS bound to the protein surface at each ANS concentration, the data were adjusted to an approximate Scatchard plot according to the equation:

$$\frac{\Delta FI}{\text{ANS}} = n \times \text{Pt} \times K_a - \Delta FI \times K_a \quad (2)$$

where ANS is the ANS concentration in each sample in μ M and Pt is the protein concentration in mg/mL.

With this Scatchard plot, K_a and n were estimated, with the K_a obtained being very similar to that calculated from Eq. 1.

The Ho is proportional to ΔFI_{\max} per mg protein and therefore it was estimated from Eq. 1 by dividing A by the protein concentration of each sample (determined by the Lowry method).

2.8 Ion-Exchange Chromatography

The runs were performed in a Waters 600 E HPLC Multisolute Delivery System (pump and controller) equipped with a Waters 717 Plus Autosampler and a Waters 996 Photodiode Array Detector (Waters Corporation, Milford, MA, USA).

A Waters AP-Minicolumn 5×100 nm $1,000 \text{ \AA}$, 8- μ m preequilibrated with buffer I (20 mM Tris-HCl, pH 9.0) was used. Fifty microliters of 20 mg/mL of sample in buffer I were injected and eluted at room temperature at a flow rate of 0.5 mL/min with a linear gradient of 0–50% (v/v) of buffer II (20 mM Tris-HCl, pH 9.0, 1M NaCl). The column effluent was monitored spectrophotometrically at 210 and 280 nm.

2.9 Fluorescence Spectroscopy

The intrinsic fluorescence of the AMGp, IMGp, and ppGb proteins was determined at 25 °C in buffer B with a Perkin-Elmer LS 50B fluorescence spectrophotometer at an excitation wavelength of 290 nm (slit width, 3 nm), an emission wavelength of 310–550 nm (slit width, 3 nm), and a scanning speed of 300 nm/min. Samples at concentrations between 0.01 and 0.03 mg/mL were obtained by dilution of the initial 1 mg/mL protein solution (Lowry method).

Ten spectra (two each from five separate assays) for each protein component were averaged and used for analysis.

2.10 Influence of Urea

The intrinsic-fluorescence spectra of the AMGp, IMGp, and ppGb were obtained as described above with 0.05–0.15 mg/mL protein solutions in the presence of different concentrations of urea (0–8.85 M). Stated in brief, the protein stocks (1.00–2.50 mg/mL), a stock solution of urea (9.44 M), and buffer B were mixed in appropriate amounts to obtain the desired concentration of protein and urea and then were incubated for 3 h at room temperature (25 ± 2 °C). The final concentrations of urea in the 3-mL solutions of the quartz cuvettes (Perkin-Elmer Corp., Wellesley, MA) are indicated in the figures.

The wavelength (λ_{\max}) was plotted against the urea concentration and the data adjusted to the following equation:

$$\lambda_{\max} = \frac{(\lambda_{\max}^N - \lambda_{\max}^D)}{\left(1 - e^{\frac{(u-u_{50})}{du}}\right)} + \lambda_{\max}^D \quad (3)$$

where λ_{\max}^N and λ_{\max}^D are the λ_{\max} of the native- and completely-denatured protein spectra, respectively, u_{50} is the urea concentration when the protein is 50% unfolded, and u is the urea concentration at a given point.

The indices IU₅₀, the molar urea concentration sufficient to reach 50% denaturation, and IU_{80/20}, the molar-concentration ratio of urea producing protein denaturations ranging from 20 to 80%, were finally calculated.

2.11 Conformational Stability (ΔG_{H_2O})

The Gibbs free energy change ΔG_D^u for the reaction.

Native (N) → Denatured (D) was estimated from the urea-denaturation curves on the assumption that the mechanism of the reaction involves only two states. In this approximation the intermediate species are not considered since they are present in very low amounts in the equilibrium. The calculations are included in Fig. 2, where f_N and f_D are the fraction of protein in the folded and unfolded conformation, respectively, so that $f_N + f_D = 1$. According to the figure, the equilibrium constant (K_D^u) and the Gibbs-free-energy change (ΔG_D^u) of the reaction at each urea concentration (u) can be calculated by means of Eqs. 4 and 5, respectively:

$$K_D = \frac{f_D}{(1 - f_D)} = \frac{f_D}{f_N} = \frac{(\lambda_{\max}^N - \lambda_{\max})}{(\lambda_{\max} - \lambda_{\max}^D)} \quad (4)$$

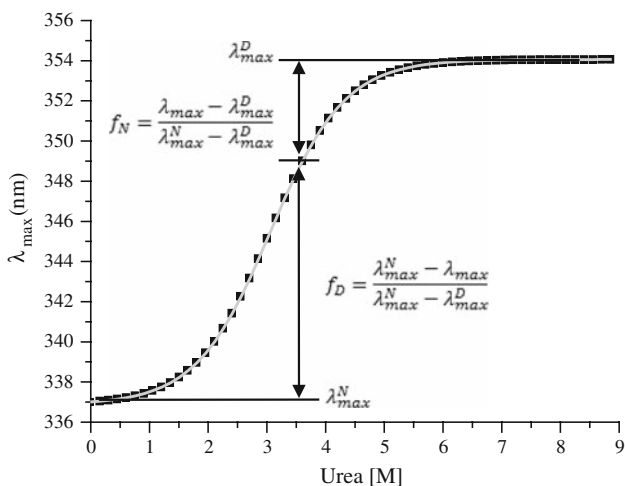


Fig. 2 Determination of the fractional amounts of native and denatured proteins with respect to the total by means of fluorescence spectroscopy

$$\Delta G_D = -RT \ln(K_D) = -RT \ln \left(\frac{\lambda_{\max}^N - \lambda_{\max}}{(\lambda_{\max} - \lambda_{\max}^D)} \right) \quad (5)$$

where, R is the gas constant in kcal/K mol and T the temperature in degrees Kelvin (K).

To estimate the ΔG_{H_2O} , the values of K_D^u obtained as described were plotted against the corresponding urea concentration and the resulting curve extrapolated to zero.

2.12 IEF→SDS-PAGE

The first dimension was performed on 18-cm linear IPG strips (pH 3–10; GE Healthcare, Milan, Italy). The strips were rehydrated with 340 μ L of rehydration buffer (7 M urea, 2 M thiourea, 2% [v/v] CHAPS, 20 mM dithiothreitol (DTT), 0.5% [v/v] IPG and 0.002% [w/v] bromophenol blue) containing 100 μ g of protein sample. The strips were focussed by means of the Multiphor II electrophoresis unit (Amersham Biosciences, Uppsala Sweden). The voltage settings for isoelectric focussing were 500 V for 1 h, 1,000 V for 1 h, and 8,000 V for 4 h up to a final condition of 30,000 V/h.

Before running the strips in the second dimension, they were incubated in equilibration buffer (2% [w/v] SDS, 6 M urea, 50 mM Tris–HCl pH 8.8, 30% [v/v] glycerol, 1% [w/v] DTT, and 0.01% [w/v] bromophenol blue) for 1 h, followed by equilibration for a further 1 h with the same solution containing 2.5% [w/v] iodoacetamide instead of DTT. The strips were cut into two pieces, placed onto two gels (12% [w/v] polyacrylamide with a stacking gel of 4% [w/v] polyacrylamide) in minislabs (BioRad Mini Protean II Model). Runs were carried out according to the Laemmli method as modified by [29]. All gels were fixed and stained with Coomassie Brilliant Blue. Molecular masses of polypeptides were calculated through the use of the low-molecular-weight protein standards (Amersham Bioscience, Uppsala Sweden).

2.13 In-Gel Enzymatic Digestion of Proteins

The protein spots indicated in Fig. 3 were excised and washed with 25 mM NH_4HCO_3 , followed by dehydration with 50% (v/v) acetonitrile in 25 mM NH_4HCO_3 . The proteins therein were then reduced with 10 mM DTT and alkylated with 55 mM iodoacetamide. The gel bands were further washed and dehydrated as described above and finally dried in a vacuum centrifuge. The proteins were digested overnight at 37 °C by addition of 15 μ L of trypsin (Promega, Madison, WI, USA, 12.5 ng/ μ L in 25 mM NH_4HCO_3).

The resulting peptide mixture was acidified with 1% (v/v) formic acid and stored at –20 °C until analysis.

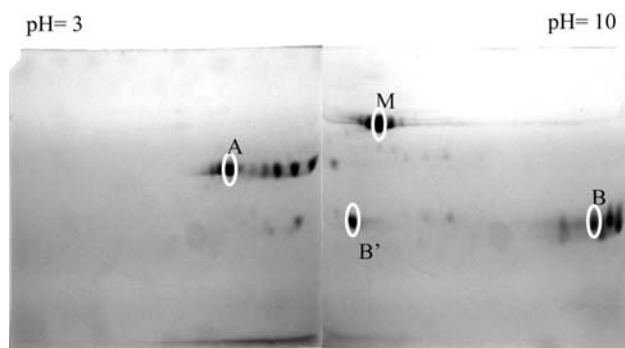


Fig. 3 Two-dimensional IEF-SDS-PAGE analysis of the globulin-p aggregates (the AMGp). The spots indicated by circles are the polypeptides that were analyzed: *M*, the propolypeptide; *A*, the acid polypeptide; *B* and *B'*, the basic polypeptides

2.14 Mass Spectrometry

Mass-spectrometry analyses were conducted by the platform “Biopolymers-Interaction-Structural Biology” located at the INRA Center of Angers-Nantes, France (http://www.angers-antes.inra.fr/plateformes_et_plateaux_techniques/plateforme_bibs).

Protein identification was first attempted by the peptide-mass-fingerprint approach by means of MALDI-TOF mass spectrometry. Analyses were performed with a MALDI LR instrument equipped with a conventional 337-nm laser (Micromass/Waters). One microliters of the sample was mixed with 1 μ L of the matrix preparation (2.5 g/L α -cyano-4-hydroxycinnamic acid, 2.5 g/L 2,5-dihydroxybenzoic acid, 70% [v/v] acetonitrile, and 0.1% [w/v] trifluoroacetic acid) and deposited onto the MALDI sample probe. Mass-data acquisitions were piloted by the Mass Lynx software (Micromass/Waters).

LC-MS/MS analyses were further performed, through the use of a Switchos-Ultimate II capillary LC system (LC Packings/Dionex, Amsterdam, the Netherlands) coupled to a hybrid quadrupole orthogonal acceleration time-of-flight mass spectrometer (Q-TOF Global, Micromass/Waters, Manchester, UK). Chromatographic separation was conducted on a reverse-phase capillary column (Pepmap C18, 75- μ m \times 15-cm, LC Packings) with a linear gradient from 2 to 40% (v/v) acetonitrile in 50 min, followed by an increase to 50% acetonitrile within 10 min, at a flow rate of 200 nL min⁻¹.

Mass-data acquisitions were piloted by the Mass Lynx software (Micromass/Waters): the MS data were recorded for 1 s on the mass-to-charge (m/z) range 400–1,500, after which time the three most intense ions (doubly, triply, or quadruply charged) were selected and fragmented in the collision cell (MS/MS measurements).

2.15 Protein Identification—Databank Searching from LC-MS/MS Data

Raw data were processed by means of the Protein Lynx Global Server v. 2.1 software (Micromass/Waters).

Protein identification was performed by comparing the collected LC-MS/MS data against Uniprot databank restricted to Viridiplantae species (release May, 26, 2009; 674,044 sequences). The mass tolerance was set at 150 ppm for parent ions (MS mode) and 0.3 Da for fragment ions (MS/MS mode), and one missed cut per peptide was allowed.

Databank searches were performed through the use of the Mascot server v. 2.2 program (Matrix Science).

2.16 Validation of Protein Identifications

For MS/MS experiments, the validation of proteins was first performed by setting the requirements to a minimum of two MS/MS spectra matching the databank sequence with individual MASCOT ion scores above the significance threshold (threshold score of 43, $p < 0.05$). These validation criteria yielded a protein identification for only spot B (entry #Q38712). The protein identifications generated by single MS/MS spectra were then considered (again setting the threshold score for an individual ion at 43). These single spectrum hits were validated only if the expected value was below 0.005 and/or when the MS/MS spectra displayed a wide series of intense fragments that, in turn, could be assigned to major predicted fragments (i.e., b or y ions) of the proposed peptide sequence. This enabled the protein identification of spot B' (entry #Q38712).

All the remaining MS/MS spectra, which runs could not be assigned to any protein after databank searching, were subjected to a *de-novo* sequencing through the use of Protein Lynx Global Server v. 2.1 software. The results were fed into the program OVNIp (<http://www.appli.nantes.inra.fr:8180/OVNIp/>) which enhance the confidence in protein identification by increasing the sequence coverage. This tactic provided four additional peptides aligned to entry #Q38712 in spot B' and four additional peptides to entry #Q38712 in spot B, thus corroborating the #Q38712 identifications in both instances.

All nonaligned *de-novo* sequences were further submitted to a sequence-homology search by means of the MS-BLAST program, with the PAM30MS matrix and the NrDB95 databank provided on the MS-BLAST server located at EMBL (released on March 17, 2005: 2,078,555 entries) [36]. The protein sequences producing high-scoring segment pairs were considered. This approach revealed two protein hits in spot A, two additional protein hits in

spot B', and one further protein hit in spot B (see "Results").

2.17 Statistical Analysis

Data were analyzed for significance (One-way ANOVA) by means of the SPSS 11.0 program (SPSS Inc., Chicago, IL). Fisher's protected LSD ($p < 0.05$) values were calculated for the appropriate data.

3 Results and Discussion

Upon consideration of the solubility of globulins (the Gb and the Gp) in extracting solvents [24], we tested the solubility at low and high ionic strength of the isolated components of the Gp (individual molecules, IMGp, and aggregates, AMGp) and of the partially purified ppGb. We found that only the AMGp exhibited a low solubility at high ionic strength; the IMGp and the ppGb showed the same solubility at both high and low ionic strength, though the solubility of the ppGb in both media was higher than that of the Gp components (Table 1). This result suggests that the AMGp may be responsible for the different properties of the Gp during protein extraction.

Size-exclusion chromatography of the samples (Fig. 4a) showed that the ppGb eluted as a main peak at a similar volume to that of the IMGp, whereas the AMGp profile indicated that these species are comprised of larger molecules of different sizes. The ND-PAGE profiles (Fig. 4b) revealed that the AMGp aggregates ran as low-mobility bands that corresponded to high-molecular-weight molecules. The IMGp pattern contained a faint band with the same mobility as one of the AMGp bands, which molecules may correspond to small aggregates. The IMGp pattern showed a major wide band of higher mobility comprising several species some of them running at the same level as the ppGb band. This last fraction also contains some species running faster than all the others that, according to results not shown (manuscript in preparation), may

correspond to the 7S globulin-like protein. Neither the 7S nor the 11S-globulin could be distinguished by chromatography in ppGb preparation.

In surveying the properties that account for the difference in the solubility behavior of the amaranth globulins—the Gp and the Gb—we determined the Ho of the molecules using the fluorescent probe ANS. The parameters obtained—Ho, the affinity constant (Ka), and the number of exposed attachment sites per mg of protein (n)—are summarized in Table 2. According to these results, the three protein species exposed a similar Ho and n sites but the Ka of the AMGp was lower than that of the IMGp and the ppGb ($p < 0.05$). This result suggested that, though the AMGp exposed the same number of ANS-attachment sites as the ppGb and the IMGp, these sites are not the same ones qualitatively (in terms of their amino-acid composition). This minor difference could be explained if a portion of the IMGp surface were inside the aggregates. Nevertheless, the composition of the ppGb would indicate that the 7S and 11S-globulins have a similar Ho to that of the IMGp.

Gorinstein et al. [16] found that the Gp Ho was higher than that of the salt-soluble globulins (Gb). These results are not in accordance with our present findings, a discrepancy which may have arisen because we are dealing with purified Gp species. The experiments of [19], however, were unsuccessful in measuring globulin Ho with the ANS probe, and this inability was attributed to the large amount of charged surface groups on the globulins.

Accordingly, when we analyzed the surface charge of the globulins by ion-exchange chromatography (Fig. 5), the profiles showed that the main peaks of ppGb and the IMGp (Fig. 5 void arrow) eluted at the same salt concentration ($\text{NaCl} = 0.44 \text{ M}$), whereas the main peak of the AMGp (Fig. 5 black arrow) eluted at a higher salt concentration ($\text{NaCl} = 0.50 \text{ M}$), thus indicating a more plentiful number of negative charges. Once again the ppGb and the IMGp exhibited a similar behavior.

We investigated conformational differences among the globulins by means of fluorescence spectroscopy (Fig. 6). According to the value of the wavelength of maximum emission (Fig. 6, inset), most of the tryptophan residues of the three globulins would be located on the surfaces of the proteins in contact with water molecules of lower mobility than free water since they pertain to tryptophan spectroscopic type II ($\lambda_{\text{max}} = 340\text{--}342 \text{ nm}$, width = $53\text{--}55 \text{ nm}$, [28]). The fluorescence emission of the ppGb was different from that of the IMGp and the AMGp ($p < 0.05$), with a higher wavelength at maximum emission (λ_{max}) and a lower maximum intensity (IF_{max} ; Fig. 6, inset). These results may be interpreted as indicating that the ppGb tryptophan residues are in an environment that is more hydrophilic—i.e., closer to the surface—than in the other globulins. The lower IF_{max} of the ppGb spectra could also

Table 1 Solubility of purified globulins in low (buffer B) and high (buffer A) ionic strength

Globulin	Solubility (%)	
	Buffer B	Buffer A
AMGp	81 ± 3^a	7.7 ± 0.1^b
IMGp	77 ± 1^c	76 ± 2^c
ppGb	92 ± 7^d	92 ± 4^d

Different letters mean significant differences ($p < 0.05$)

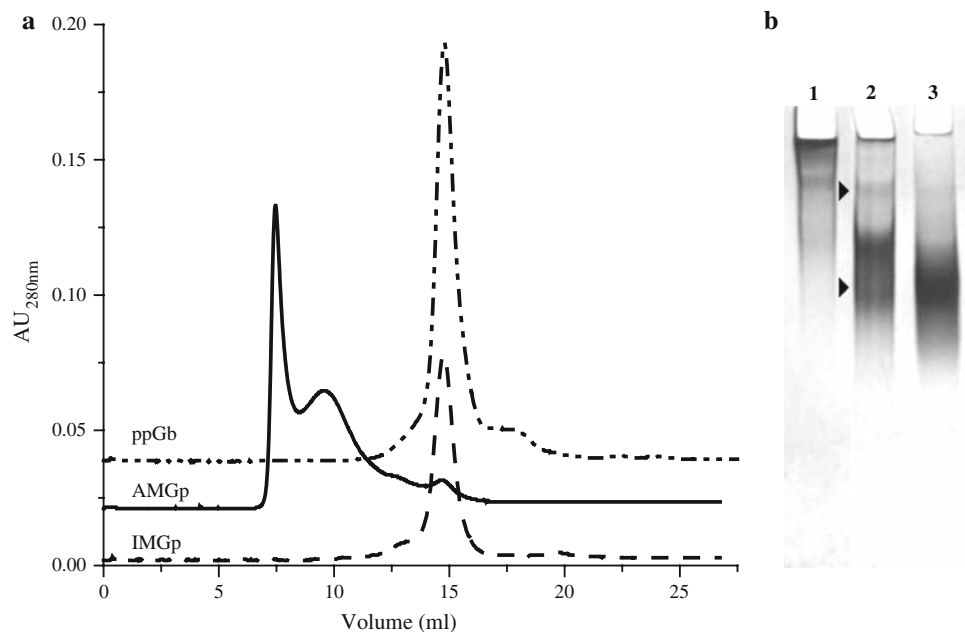


Fig. 4 **a** Gel-filtration chromatography and **b** ND-PAGE of: AMGp (1), IMGp (2) and ppGb IM, (3)

Table 2 Surface hydrophobicity parameters of purified globulins

Fraction	H_0^*	K_a^{**}	n^{***}
AMGp	1,655 ^a	0.042 ^a	1,571 ^a
IMGp	1,808 ^a	0.080 ^b	1,856 ^a
ppGb	1,512 ^a	0.070 ^b	1,512 ^a

* Surface hydrophobicity: IF/mg/ml protein, ** Affinity constant: 1/ μ M, *** Attachment sites/mg protein. Different letters in the same column mean significant differences ($p < 0.05$)

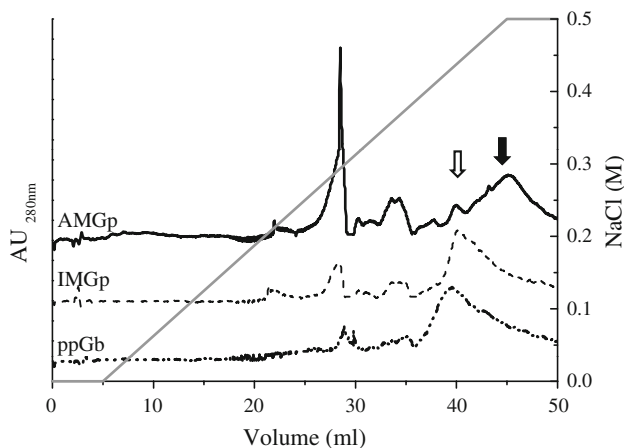


Fig. 5 Ion-exchange HPLC of the ppGb, the AMGp, and the IMGp

be the consequence of a different number of tryptophan residues in the ppGb than in the IMGp and the AMGp. Nevertheless, the IMGp and AMGp did not show significant differences between their spectra. The ppGb λ_{\max} agrees with the value indicated by [16] for the amaranth

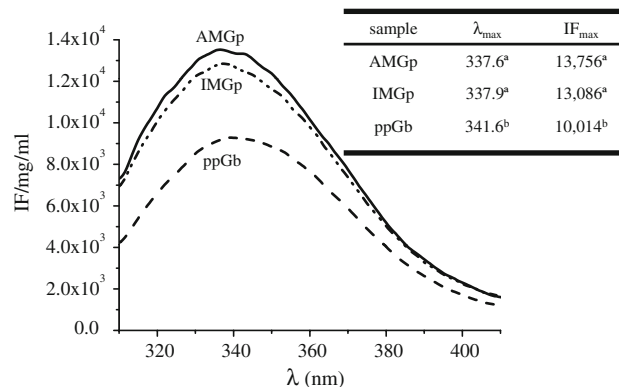


Fig. 6 Fluorescence-emission spectra of the globulins standardized to 1 mg/ml, with excitation at 295 nm. Inset: IF_{\max} , maximum fluorescence-emission intensity; λ_{\max} , wavelength of maximum fluorescence intensity. ppGb salt soluble globulins, AMGp globulin-p aggregates, IMGp globulin-p individual molecules

nonpurified globulin fraction, although their results are not in accordance with the present studies in that they found the Gp (referred to as albumin-2) to have more greatly exposed tryptophans. This disagreement could also result from differences in the degree of purification of the proteins analyzed between the two studies.

Through the use of fluorescence spectroscopy we studied the conformational stability of the globulins in a test of the denaturing influence of urea. As expected, the spectra of the three globulins obtained at increasing urea concentrations exhibited a shift of λ_{\max} to longer wavelengths, thus indicating a progressive unfolding and exposure of tryptophan residues on the protein surface. The relationship

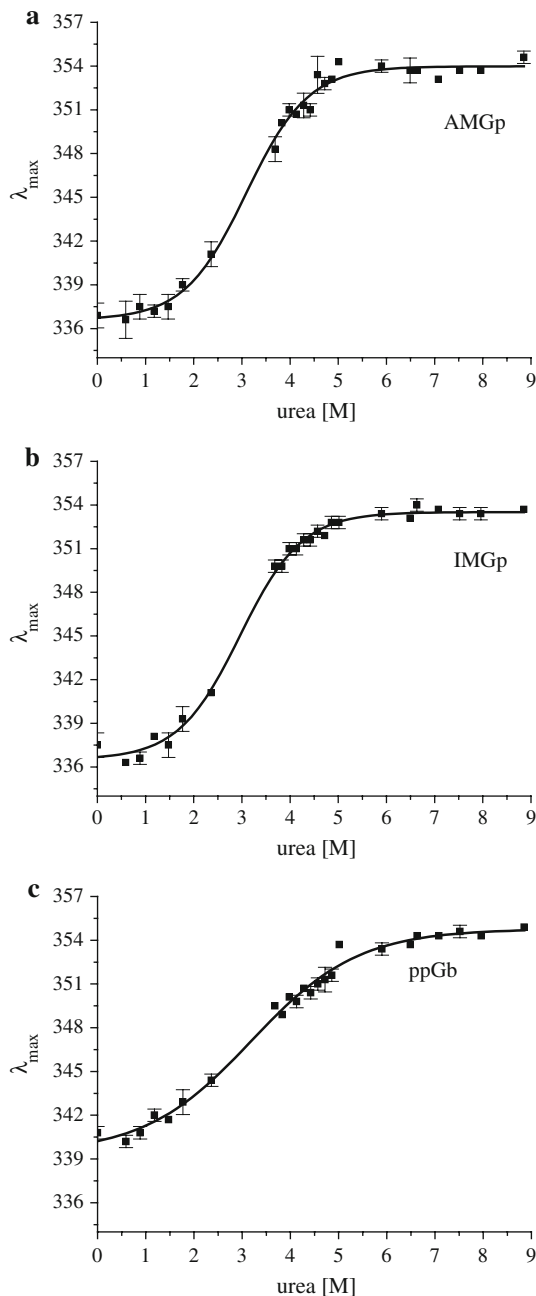


Fig. 7 Effect of urea concentration on the wavelength of maximum fluorescence-emission intensity (λ_{max}). **a** AMGp globulin-p aggregates; **b** IMGp globulin-p unitary molecules, **c** ppGb salt soluble globulins

between the λ_{max} of the spectra and the corresponding urea concentration is depicted in Fig. 7 along with the fitted sigmoid curves. On the basis of these data, we calculated the parameters shown in Table 3. The IU_{50} values of the three globulin species were similar, while the AMGp and the IMGp $IU_{80/20}$ value was lower than that of the ppGb ($p < 0.05$), suggesting a higher cooperativity during the process of denaturation with the AMGp and the IMGp than

Table 3 Denaturation of globulins by urea

Globulin	IU_{50}^*	$IU_{80/20}^{**}$	$\Delta G_{H_2O}^{***}$
AMGp	3.09 ^a	1.813 ^a	3.1 ^a
IMGp	3.00 ^a	1.860 ^a	2.9 ^a
ppGb	3.19 ^a	2.900 ^b	2.2 ^b

Indices and Gibbs free energy

* Urea concentration at 50% denaturation (M), ** urea-concentration ratio producing denaturation from 20 to 80%, *** free energy of denaturation (kcal/mol). Different letters in the same column mean significant differences ($p < 0.05$)

with the ppGb. As the temperature was not stringently controlled (25 ± 2 °C), the ΔG_{H_2O} obtained must be considered only an approximate value; though the results may nevertheless be compared and clearly pointed to a significant difference between the AMGp or the IMGp, and the ppGb ($p < 0.05$). Moreover, the Gibbs free energy of unfolding was the same for the AMGp and the IMGp but was higher for those species than that of the ppGb (Table 3). According to these results the Gp molecules showed a more compact structure and a higher conformational stability than the Gb. Because of the presence of the two types of globulins (the 7S and the 11S) in the ppGb preparation, these differences could account for this heterogeneity.

From the above results and the published information cited, the Gp and the 11S-globulins would appear to correspond to two isoforms of the amaranth 11S-globulins that arise from polypeptide segregation during oligomer formation. To investigate this possibility we compared the sequences of the AMGp polypeptides (M, the propolypeptide; A, the acid polypeptide; and B and B', the basic polypeptides, Fig. 3) to the reported sequences of the 11S propolypeptide.

In the first attempt to this end, a conventional proteomics approach was used in which protein identity was assessed by comparison to reported sequences in the Uniprot databank pertaining to green plants. Three procedures were subsequently employed: namely, error-intolerant databank search, then tentative alignment of *de-novo*-generated stretches of amino acids, and finally MS-BLAST search of the remaining spectra.

The protein assignment was made following Nesvizhskii and Aebersold's adaptation of the parsimony principle [27] which approach led to the list of proteins shown in Table 4.

From these MS analyses and databank searches, we find it difficult to deduce the complete amino-acid sequences of the polypeptides, mainly because it is likely that none of the reported sequences describes exactly the polypeptide sequence contained in our isolated spots. A functional description of the major components of the spots could be assessed, however, through pure similarity. Therefore, the

Table 4 Protein assignment to trypsin-digested globulin-p polypeptides analyzed by MS

SPOT #	ID method used (a)	Accession number	Description	Species	MW	Score (b)	Number of peptides
Spot A	MS-BLAST	Q9SE84	Legumin-like protein	<i>Perilla frutescens</i>	52735	270	6
	MS-BLAST	P09800	Legumin B	<i>Gossypium hirsutum</i>	58709	113	2
Spot B'	MASCOT DB search	Q38712	11S-globulin (fragment)	<i>Amaranthus hypochondriacus</i>	57035	59	1
	OVNIp de novo alignment	Q38712	11S-globulin-seed storage-protein (fragment)		57035	218	4
	MS-BLAST	Q9AUD2	11S-globulin	<i>Sesamum indicum</i>	56588	256	5
	MS-BLAST	Q40347	Globulin	<i>Magnolia salicifolia</i>	53663	89	2
Spot B	MASCOT DB search	Q38712	11S-globulin (fragment)	<i>Amaranthus hypochondriacus</i>	57035	371	7
	OVNIp de novo alignment	Q38712	11S-globulin seed-storage protein (fragment)		57035	249	4
	MS-BLAST	Q40347	Globulin	<i>Magnolia salicifolia</i>	53663	380	8
Spot M	MS-BLAST	P09800	Legumin B	<i>Gossypium hirsutum</i>	58709	168	4

The Nesvizhskii and Aebersold parsimony principle adaptation was observed

spots A and M could likely be assigned to legumin-like proteins different from the *Amaranthus* species, while the spots B and B' could contain the beta-subunit of the amaranthus-globulin propolypeptide (gil122726601; Table 4).

Though these results are not conclusive, they do show that the M propolypeptide is different from the reported for the salt-soluble 11S-globulin. Moreover, our findings also suggest that the A and B polypeptides are not the products of the 11S-globulin-propolypeptide hydrolysis. The different amino-acid compositions of the 11S-globulin and the Gp polypeptides may be the cause of the Gp's tendency to aggregate. When the A and B polypeptides were compared with the M propolypeptide, no match was found, indicating that neither of these two species came from that particular precursor. These results underscore the polymorphism of amaranth globulins.

4 Conclusions

Few laboratories [3, 8–10, 15–17, 23, 24] have described Gp (or albumin-2) as a fraction different from the 11S-globulin, thus suggesting that the differences between the two fractions were subtle. The Gp was distinguished from the other globulins by its solubility properties, and, according to results of this study, the AMGp aggregates are responsible for those distinguishing properties. A possible explanation for the solubility characteristics of the aggregates might be attributed to the large negative charge these molecules expose, as demonstrated by ion-exchange analysis. The resulting charge repulsion would allow the aggregates to be dissolved in alkaline media at low ionic strength; but the charge screening at a higher degree of

salinity would allow hydrophobic interactions leading to a lack of solubility. Our results show that the AMGp aggregates presented hydrophobic patches with a lower affinity for the fluorescent probe ANS; but, considering that this probe is an anion and that the AMGp exposed a larger overall negative charge, such a result is not conclusive and we therefore cannot discard the above hypothesis.

Finally, we have demonstrated sequence differences between the AMGp polypeptides and the reported amaranth 11S-globulin propolypeptide (gil122726601). These differences suggest that the Gp and the 11S-globulin consist in two 11S-globulin isoforms generated by polypeptides coming from different legumin-gene subfamilies.

Acknowledgments The authors wish to thank Dr. Donald F. Haggerty, a retired career investigator and native English speaker, for editing the final version of the manuscript.

References

1. Abugoch LE, Martínez EN, Añón MC (2003) *J Agric Food Chem* 51:4060–4065
2. Adachi M, Kanamori J, Masuda T, Yagasaki K, Kitamura K, Mikami B, Utsumi S (2003) *PNAS* 100:7395–7400
3. Aphalo P, Castellani OF, Martínez EN, Añón MC (2004) *J Agric Food Chem* 52:616–622
4. Aphalo P, Martínez EN, Añón MC (2009) *Protein J* 28:131–138
5. Barba de la Rosa A, Paredes-López O, Gueguen J (1992) *J Agric Food Chem* 40:937–940
6. Barba de la Rosa AP, Herrera-Estrella A, Utsumi S, Paredes-López O (1996) *J Plant Physiol* 149:527–532
7. Cardamone M, Puri NK (1992) *Biochem J* 282:589–593
8. Castellani OF, Martínez EN, Añón MC (1998) *J Agric Food Chem* 46:4846–4853
9. Castellani OF, Martínez EN, Añón MC (1999) *J Agric Food Chem* 47:3001–3008

10. Castellani OF, Martínez EN, Añón MC (2000) *J Agric Food Chem* 48:5624–5629
11. Chen S, Paredes-López O (1997) *J Food Biochem* 21:53–65
12. Fukushima D (1991) *Food Rev Intl* 7:353–381
13. Gorinstein S, Zemser M, Paredes-López O (1996) *J Agric Food Chem* 44:100–105
14. Gorinstein S, Zemser M, Friedman M, Vasco-Méndez NL, Paredes-López O (1996) *J Agric Food Chem* 44:93–99
15. Gorinstein S, Jaramillo NO, Medina OJ, Rogrigues WA, Tosello GA, Paredes-López OJ (1999) *Prot Chem* 18:687–693
16. Gorinstein S, Delgado-Licon E, Pawelzik E, Permady HH, Weisz M, Trakhtenberg S (2001) *J Agric Food Chem* 49:5595–5601
17. Konishi Y, Horikawa K, Oku Y, Azumaya J, Nakatani N (1991) *Agric Biol Chem* 55:2745–2750
18. Marcone MF, Yada RY (1991) *Agric Biol Chem* 55:2281–2289
19. Marcone MF, Yada RY (1992) *J Agric Food Chem* 40:385–389
20. Marcone MF, Beniac DR, Harauz G, Yada RY (1994) *J Agric Food Chem* 42:2675–2678
21. Marcone MF, Kakuda Y, Yada RY (1998) *Food Chem* 63:265–274
22. Marcone MF, Yada RY (1998) *Food Chem* 61:319–326
23. Martínez EN, Añón MC (1996) *J Agric Food Chem* 44:2523–2530
24. Martínez EN, Castellani OF, Añón MC (1997) *J Agric Food Chem* 45:3832–3839
25. Medina-Godoy S, Valdez-Ortiz A, Valverde E, Paredes-López O (2006) *Biotechnol J* 1:1082–1085
26. Molina MI, Circosta A, Añón MC, Petruccelli S (2008) *Phytochem* 69:58–65
27. Nesvizhskii AI, Aebersold R (2005) *Mol Cell Proteomics* 4:1419–1440
28. Permyakov EA (1993) In *luminiscent spectroscopy of proteins*. CRC Press, Boca Raton, pp 35–56
29. Petruccelli S, Añón MC (1994) *J Agric Food Chem* 42:2161–2169
30. Petruccelli S, Molina MI, Lareu FJ, Circosta A (2007) *Plant Physiol Biochem* 45:400–409
31. Plietz P, Drescher B, Damaschun G (1987) *Intl J Biol Macromol* 9:161–165
32. Quiroga AV, Martínez EN, Añón MC (2007) *Protein J* 26:327–333
33. Romero-Zepeda H, Paredes-López OJ (1996) *Food Chem* 19:329–339
34. Salnikow J, Zemser M, Gorinstein S, Friedman M, Scheler CH, Paredes-López O (1998) *Protein J* 17:543–545
35. Segura Nieto M, Barba de la Rosa AP, Paredes-López O (1994) In: Paredes-López O (ed) *Amaranth biology, chemistry and technology*. CRC Press, Boca Raton, pp 75–106
36. Shevchenko A, Sunyaev S, Loboda A, Shevchenko A, Bork P, Ens W, Standing KG (2001) *Anal Chem* 73:1917–1926
37. Vasco-Méndez NL, Paredes-López OJ (1995) *Food Chem* 18:227–238